Outer Loop Requirements for Vertical Lift Unmanned Aerial System Automated Flying Qualities

Christina M. Ivler
Associate Professor of Mechanical Engineering
University of Portland
Portland, Oregon

William P. Geyer Jr.
Academic Instructor
United States Naval Test Pilot School
Patuxent River, Maryland

ABSTRACT

An unmanned aerial system automation qualities framework (previously known as the unmanned aerial system handling qualities framework) has been in development to determine a set of criteria and mission task elements for evaluating the airworthiness of unmanned aerial systems. The framework is being developed to apply across a range of unmanned aircraft from Group 1 to Group 4-5, via scalable predicted (quantitative) automation qualities metrics as well as scalable mission task elements. Prior work has developed scalable mission task elements and predictive attitude response criteria, scaled from MIL-DTL-32742 (which supersedes ADS-33E-PRF). This paper extends the UAS automation qualities framework to provide predictive (quantitative) criteria for velocity and position responses. The paper evaluates Froude scaled velocity disturbance rejection bandwidth and position disturbance rejection bandwidth requirements from MIL-DTL-32742 and describes and evaluates two new metrics, velocity bandwidth and tracking bandwidth, as possible new criteria. These metrics are defined in the paper and were evaluated as predictive quantities for automation handling qualities level using lateral reposition and depart/abort mission task elements. The evaluation was conducted by modifying the control system to achieve parametric variation of the metrics of interest and then assessing the performance with simulation and flight test of mission task elements. Three small unmanned vertical lift aircraft were used in this study; the University of Portland hexacopter, the USNTPS X8-M coaxial quadcopter and Synergy 626 single main rotor helicopter. It was found that the newly defined tracking bandwidth and velocity disturbance rejection bandwidth are key predictive criteria for automation qualities level for automated mission task elements on the test aircraft.

NOTATION

A, B	State-space matrices
J_{mf}	Model following cost
N	Froude scale characteristic length ratio
NED	North, East, Down coordinate frame
p, q, r	Angular rates of rotation (rad/s)
$\mathrm{p_x}, \mathrm{p_y}, \mathrm{p_z}$	Positions expressed in the level-heading coordinate frame (ft)
$\mathrm{v_x}, \mathrm{v_y}, \mathrm{v_z}$	Velocities expressed in the level heading coordinate frame (ft/s)
ϕ, θ, ψ	Euler angles (rad)
ω_c	Cross-over frequency (0 db) of open-loop response (rad/s)
ω_{DRB}	Disturbance rejection bandwidth (rad/s)
$\omega_{T_{BW}}$	Tracking bandwidth (rad/s)
λ	Eigenvalues (rad/s)

Acronyms

BW	Bandwidth
DRB	Disturbance Rejection Bandwidth
DRP	Disturbance Rejection Peak
eVTOL	Electric Vertical Take-Off and Landing
L1	Level 1
L2	Level 2
MTE	Mission Task Element
UAS	Unmanned Aerial System
UP	University of Portland
USNTPS	United States Naval Test Pilot School
VTOL	Vertical Take-Off and Landing

Presented at the Vertical Flight Society's 80th Annual Forum & Technology Display, Montréal, Québec, Canada, May 7-9, 2024.

INTRODUCTION

In the military and commercial sectors, it is widely acknowledged that criteria like those used for evaluating handling qualities of manned rotorcraft, such as in MIL-DTL-32742 [1], are needed to evaluate the flying characteristics for unmanned and automated vertical take-off and landing (VTOL) aircraft. Techniques for evaluating handling qualities from MIL-DTL-32742 (which supersedes ADS-33E-PRF [2]) are now being proposed for certification of emerging electric vertical take-off and landing (eVTOL) configurations [3], and so adapting these criteria for unmanned and automated configurations is relevant for both commercial and military applications. It is necessary to obtain criteria against which to evaluate the airworthiness of existing and emerging aircraft that feature autonomy at varying levels, and may be fully unmanned or may carry passengers but have no pilot onboard. The VTOL aircraft that fall within this category can range from small VTOL unmanned aerial systems (UAS) up through large autonomous configurations that can carry multiple passengers (including eVTOL). Development of a scalable framework of vertical lift automated flying qualities criteria and mission task elements (MTEs) is important to ensure that the methods can be applied across the wide range of aircraft sizes and configurations (multicopters, single rotor helicopter, tiltrotors, etc.) that encompass aircraft that range from small UAS (Group 1) up through full scale autonomous aircraft (Group 4-5) that could potentially carry passengers.

A proposed scalable UAS handling qualities framework has been developed by the University of Portland (UP), in collaboration with the US Army Combat Capabilities Development Command [4, 5, 6] and United States Naval Test Pilot School (USNTPS) [7]. Recently, we have come to refer to this set of requirements as automated flying qualities requirements, as opposed to UAS handling qualities requirements, largely inspired by the work of Klyde [3]. The framework includes a range of scalable automated MTEs, some adapted from ADS-33E-PRF and some developed specifically for UAS [4]. The automated MTEs provide assessment of the automation qualities level, which was previously referred to as the unmanned handling qualities level. Regardless of the name, this framework has been used to validate predictive Froude-scaled metrics such as disturbance rejection bandwidth (DRB), attitude bandwidth (BW) and damping ratio, with Froude-scaled MTEs for small (<55 lb) UAS. This Froude-scaled framework was proven via cross-correlation of scaled predictive flying qualities metrics and automated MTE performance of the IRIS+ quadcopter [6], the University of Portland hexacopter (DJI F550 frame) [4, 5], Synergy 626 single main rotor helicopter [4, 7] and the USNTPS X8-M, a coaxial quadcopter [7]. The framework has been evaluated at a range of mission gross weights, from empty to heavy [7] and is robust to gross weight variations within group 1 UAS.

Missing from the framework are criteria for the outer-loop velocity and position closed-loop BW and/or DRB. In prior work of Refs. [4, 7], attitude BW and attitude DRB were evaluated as predictive criteria for automation qualities. It was found that these attitude criteria scaled well using Froude scaling from ADS-33E-PRF, and that the scaled Level 1 criteria from ADS-33E-PRF was well correlated with Level 1 performance in scaled, automated MTEs. However, given that there are also velocity and position feedback in place during the automated MTEs, the role of velocity BW and position BW versus attitude BW in achieving desired performance was unknown. Parametric variation in velocity and position BW and DRB were not explicitly explored in prior work, although the velocity and position loops were designed to meet Froude-scaled Level 1 DRB recommendations from Ref. [8]. This work seeks to evaluate the importance of the outer (velocity/position) loop characteristics in achieving Level 1 automation qualities through simulation and flight testing of three different Group 1 UAS that have been evaluated in prior studies, the University of Portland hexacopter, the Synergy 626 single main rotor helicopter and the USNTPS X8-M coaxial quadcopter.

TEST VEHICLES AND SIMULATION MODELS

The three Group 1 UAS evaluated for this research were selected due to their varied size and configuration. These aircraft are described in the following sections of the paper.

UP Hexacopter

The University of Portland (UP) hexacopter, shown in Figure 1a, was used as a test bed for this research. The UP hexacopter is based on a Flamewheel F550 frame and has a 1.8 ft hub-to-hub distance. Flight-accurate state-space models of the vehicle have been previously developed at hover/low-speed for the 3.75 lb empty configuration and for the 5.5 lb mission configuration using the CIFER® system identification method [9]. The flight controller is a Pixhawk 2.1 (Hex Cube Black) autopilot with Arducopter version 4.0 [10] with a custom control mode that is developed in Simulink and then integrated as a flight mode into the codebase [11]. The mission configuration (5.5 lb) was used for this research.

Synergy 626

The Synergy 626 helicopter, shown in Figure 1b was also used as a test bed for this research. This UAS has a fuselage length of 3.56 ft, and a rotor diameter of 4.57 ft. Previous research was conducted in the empty configuration, 10 lb, and the mission configuration, 14.3 lb. The helicopter rotor is a two-bladed teetering design that uses rubber collars on the spindle to provide flapping stiffness. The effective offset was estimated to be 19%. The flight controller is a CUAV Pixhawk v5 (similar to Pixhawk 2.1) with Arducopter version 4.4.4 [10]. The mission configuration was used for this research.

USNTPS X8-M Coaxial Quadcopter

The USNTPS X8-M, shown in Figure 1c, was manufactured by 3D Robotics and designed to autonomously map land using a digital camera. After post-flight processing of the digital images, the software provides a high-resolution photo of the mapped area. The aircraft is a coaxial, quadcopter x-frame configuration and has an operating weight of 7.3 lbs. The aircraft with propellers turning is 29 ¼ inches wide and 23 ¼ inches long and has a hub-to-hub distance of 1.83 ft. The flight controller is a Pixhawk 1 with Arducopter version 4.2.3 firmware [10]. A flight-accurate state-space model in hovering flight was previously developed [7] using the CIFER® system identification method [9]. The flight-accurate dynamics model was implemented into the Arducopter software-in-the-loop simulator for the simulation study.

AUTOMATION QUALITIES METRICS

This section will provide definition of the methodology by which quantitative automation (previously, UAS handling) qualities metrics are determined and defined within the context of this paper. Given that most of these metrics are adapted from manned system handling qualities metrics, it is not always clear how to translate the analysis of the automation qualities metrics within the unmanned system architecture. As such, a generic block diagram that has elements used in many unmanned control systems is provided in Figure 2 and will be used to document the methods for extracting the automation qualities metrics of interest. This generic architecture is based on a nested control system approach where velocity and position loops wrap around the attitude control loops. This is a common architecture choice for velocity and position control of rotorcraft [12]. There are two variants of the generic block diagram – one where the trajectory generator outputs target velocity commands (Figure 2a) and a second variant where the trajectory outputs target position commands (Figure 2b). These different command structures will result in the same response if all the controller blocks are the same and given equivalent desired trajectories (such that the integration of V_{target} in Figure 2a is equal to P_{target} in Figure 2b). Note that these velocity/position commands are typically provided in the North-East-Down (NED) coordinate frame and then converted to the local-vertical frame (see Figure 6, later, for definition of the local-vertical frame) at some point before they are passed to the attitude controller. The exact location where the coordinate conversion occurs varies, so is not shown on the block diagram explicitly, but must be included at some point in the block diagram if the trajectory target commands are provided in the NED frame. This block diagram is developed with the understanding that some of the elements may not be used in all control system architectures, for example certain feed forward controllers may not be present and those blocks would have an effective transfer function of zero for that case, but the inputs/output locations for the calculation of the predictive automation qualities metrics still generally apply.

(a) University of Portland Hexacopter

(b) Synergy 626

(c) *USNTPS X8-M*

Figure 1. Aircraft to be used for outer loop automation qualities study.

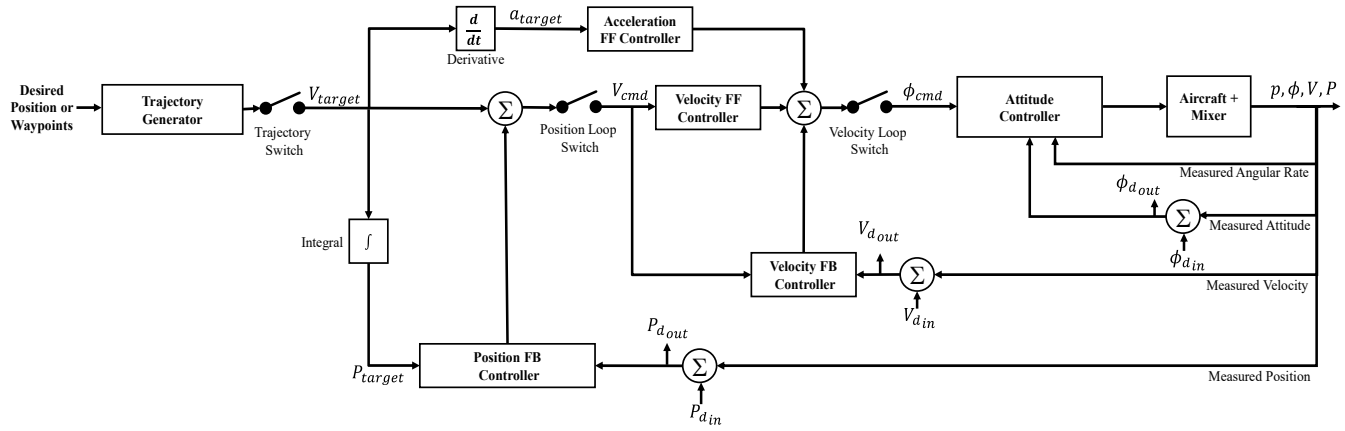

a. Velocity target command trajectory structure

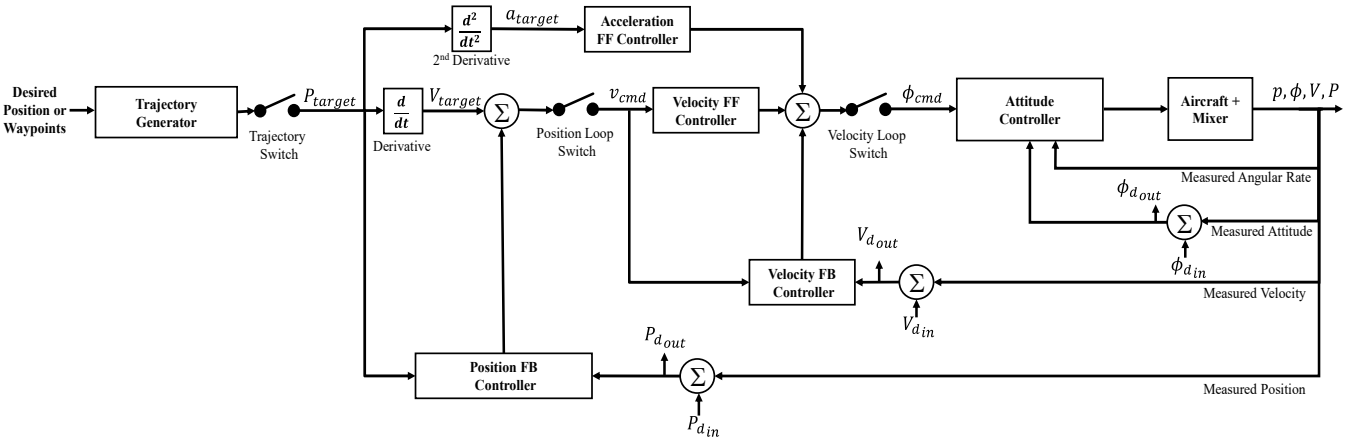

b. Position target command trajectory structure

Figure 2. Generic block diagram for trajectory following for evaluating predictive metrics.

Table 1 shows the method for calculating the bandwidth metrics that are discussed in this work, describes which switches from the block diagrams in Figure 2 are on/off during evaluation of the metric, and gives the inputs and outputs for the metric from the block diagram. The proposed Level 1/Level 2 (L1/L2) criteria boundaries for UAS are also given in the table. Note that the metrics are typically calculated at the UAS scale and then scaled up to full-scale equivalent (multiply by $\frac{1}{\sqrt{N}}$) for evaluation relative to the L1/L2 criteria. These metrics can be collected in flight via frequency sweeps for best accuracy, or alternately, via linearization of a block diagram that has been flight validated to be highly accurate (identifies metrics within $\pm 5\%$). To calculate the frequency responses of interest from time domain data, a frequency response identification tool, such as CIFER® [9] can be used.

Table 1. Predicted automation qualities metrics definitions.

Predicted Automation Qualities Metric	Full Scale L1/L2 Boundary (rad/s)	Response of Interest	Velocity Loop Switch	Position Loop Switch	Trajectory Loop Switch	Metric Calculation *multiply by $\frac{1}{\sqrt{N}}$ for full scale equivalent value*
Attitude DRB $\boldsymbol{A = \phi, \theta, \psi}$	$\omega_{\phi_{DRB}} = 0.9$ $\omega_{\theta_{DRB}} = 0.9$* $\omega_{\psi_{DRB}} = 0.7$	$\frac{A_{d_{out}}}{A_{d_{in}}}(j\omega)$	Open	Open	Open	Frequency $\omega_{A_{DRB}}$ where magnitude crosses -3dB $\left\|\frac{A_{d_{out}}}{A_{d_{in}}}(j\omega_{A_{DRB}})\right\| = -3$ dB
Velocity DRB $\boldsymbol{V = v_x, v_y, v_z}$	$\omega_{v_{x_{DRB}}} = 0.54$* $\omega_{v_{y_{DRB}}} = 0.54$ $\omega_{v_{z_{DRB}}} = 0.7$	$\frac{V_{d_{out}}}{V_{d_{in}}}(j\omega)$	Closed	Open	Open	Frequency $\omega_{V_{DRB}}$ where magnitude crosses -3dB $\left\|\frac{V_{d_{out}}}{V_{d_{in}}}(j\omega_{V_{DRB}})\right\| = -3$ dB
Position DRB $\boldsymbol{P = p_x, p_y, p_z}$	$\omega_{p_{x_{DRB}}} = 0.17$ $\omega_{p_{y_{DRB}}} = 0.17$ $\omega_{p_{z_{DRB}}} = 0.17$	$\frac{P_{d_{out}}}{P_{d_{in}}}(j\omega)$	Closed	Closed	Open	Frequency $\omega_{P_{DRB}}$ where magnitude crosses -3dB $\left\|\frac{P_{d_{out}}}{P_{d_{in}}}(j\omega_{P_{DRB}})\right\| = -3$ dB
Attitude BW $\boldsymbol{A = \phi, \theta, \psi}$	$\omega_{\phi_{BW}} = 2$** $\omega_{\theta_{BW}} = 2$** $\omega_{\psi_{BW}} = 2$**	$\frac{A}{A_{cmd}}(j\omega)$	Open	Open	Open	Frequency $\omega_{A_{BW}}$ where the phase crosses -135^o $\angle\frac{A}{A_{cmd}}(j\omega_{A_{BW}}) = -135^o$
Velocity BW $\boldsymbol{V = v_x, v_y}$	No boundary values are known/proposed	$\frac{V}{V_{cmd}}(j\omega)$	Closed	Open	Open	Frequency $\omega_{V_{BW}}$ where the phase crosses -135^o $\angle\frac{V}{V_{cmd}}(j\omega_{V_{BW}}) = -135^o$
Tracking BW (velocity command) $\boldsymbol{V = v_x, v_y, v_z}$ $\boldsymbol{P = p_x, p_y, p_z}$	Proposed values: $\omega_{T_{xBW}}$ = 0.6 rad/s $\omega_{T_{yBW}}$ = 0.6 rad/s	$\frac{P}{V_{target}}(j\omega)$	Closed	Closed	Open	Frequency $\omega_{T_{BW}}$ where the phase crosses -135^o $\angle\frac{P}{V_{target}}(j\omega_{T_{BW}}) = -135^o$
Tracking BW (position command) $\boldsymbol{P = p_x, p_y, p_z}$	Proposed values: $\omega_{T_{xBW}}$ = 0.6 rad/s $\omega_{T_{yBW}}$ = 0.6 rad/s	$\frac{P}{P_{target}}(j\omega)$	Closed	Closed	Open	Frequency $\omega_{T_{BW}}$ where the phase crosses -45^o $\angle\frac{P}{P_{target}}(j\omega_{T_{BW}}) = -45^o$

* For UAS, the pitch-axis DRB requirements for attitude and velocity have been proposed to be equivalent to the roll-axis requirements, which are significantly higher than MIL-DTL-32742 for the pitch axis.

** For UAS, the attitude boundary for "all other MTEs, UCE > 1" requirement is suggested per Ref. [7].

The attitude BW and DRB metrics described in Table 1 are extracted with similar methods to that presented in MIL-DTL-32742 [1]. For autonomous aircraft, the outer velocity and position loops are turned off by opening the velocity loop switch (the position loop switch and trajectory loop switches should also be open if there are any additional feed forward elements from those paths). This means that if data is collected via automated frequency sweep in flight test (rather than using a flight validated model linearization technique) that a remote pilot will need to actively control the aircraft so that it stays on the flight condition during the frequency sweep considering that only attitude modes will be active. Once the frequency responses of interest are determined, Figure 3 shows how to determine the DRB and disturbance rejection peak (DRP), and Figure 4 illustrates how to extract the attitude BW. These calculations are also described mathematically in the far-right column of Table 1.

Velocity DRB and velocity BW data described by Table 1 are collected with the velocity loop switch in Figure 2 closed, but with the position and trajectory loop switches open. The velocities of interest in these calculations $(\mathrm{v_x}, \mathrm{v_y}, \mathrm{v_z})$ are defined in the local-vertical axes (x, y) shown in Figure 6, where the velocities of interest are the horizontal components relative to the target heading of the vehicle. When using this coordinate frame, v_x is the horizontal velocity component pointed in the direction of the nose of the aircraft rather than the north velocity component. Since it is desired to obtain these metrics in the local-vertical axes as the aircraft layout could cause these metrics to be different between the longitudinal and lateral axes, the commands and disturbances must be made in the local-vertical axes. If this is not possible, then the heading should be aligned so that the nose is pointed north when conducting sweeps or linearizing. Then, the NED frame elements of the block diagram coincide with the level-heading frame, as shown by Figure 6 with $\psi = 0$. The velocity DRB metrics are determined from the velocity disturbance response as illustrated in Figure 3 and the velocity BW metric is extracted from the closed loop velocity response as shown by Figure 4. The velocity DRB metric is similar to that described in Section 3.3.11.1 of MIL-DTL-32742, which details short-term translational rate responses to disturbance inputs. The velocity BW method is not used in manned military specifications but is similar to the concept of attitude BW for an attitude command system, except now with the input and output being velocity rather than attitude. The velocity BW is related to the speed of the closed-loop velocity response to commanded velocity changes.

The position DRB metric is determined with methods described in Table 1 per frequency responses extracted with the trajectory loop switch in Figure 2 open, but with all other loops closed. The position disturbance input and output locations are shown in the block diagram, and the metrics are defined in the local-vertical frame, similar to the velocity metrics. Then the DRB is extracted from the response per Figure 3. The position DRB calculation is nearly identical to the position hold DRB response metric detailed in section 3.3.10.1 of MIL-DTL-32742, except that it is applied for general position tracking modes, not just for position hold modes.

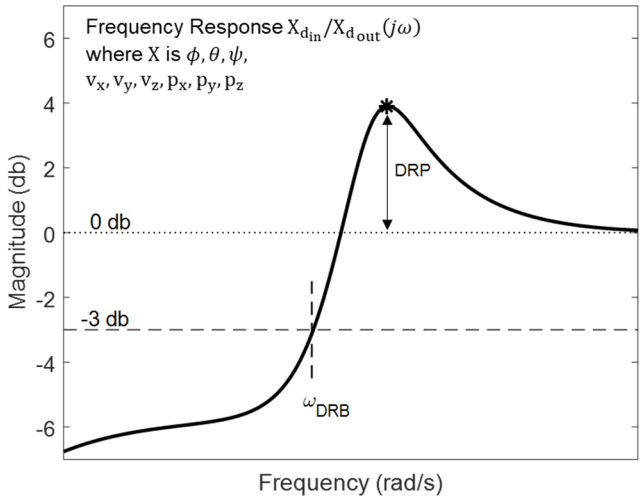

Figure 3. Calculation of disturbance rejection bandwidth and disturbance rejection peak.

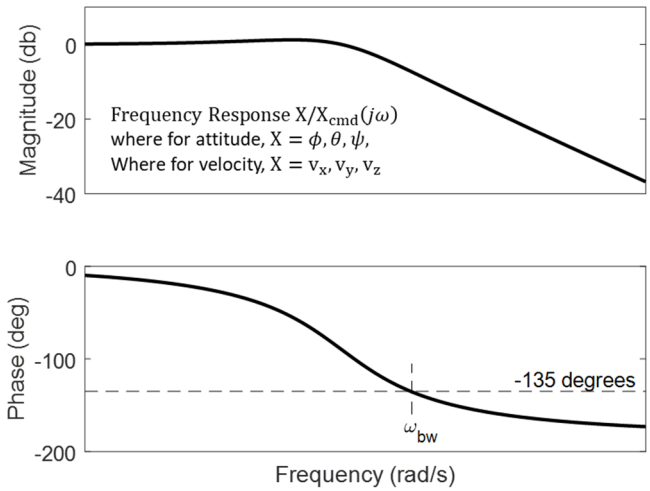

Figure 4. Calculation of attitude and velocity bandwidth.

A new metric, tracking bandwidth, describes the speed of the trajectory tracking response of the unmanned aircraft. Similar to the other velocity and position metrics, the tracking bandwidth is also defined in the local-vertical frame. This is an important metric related to the performance of the UAS autonomous MTEs. The tracking command is often passed to the controller as velocity target V_{target} as shown in Figure 2a. The -135^o phase bandwidth of the V_{target} input to the position P output, is defined as the tracking BW herein, and has been found to be a key metric in the tracking accuracy of the MTEs, as will be shown later in this work. This is analogous to a rate command system, where the pilot is commanding rate and the output of interest is its integral, attitude. Then, for example, the longitudinal tracking BW $\omega_{T_{x_{bw}}}$ can be extracted from the -135^o phase bandwidth of the $\frac{\mathrm{p_x}}{\mathrm{v_{x_{target}}}}(j\omega)$ response, as shown by the dashed line in Figure 5. By using block diagram algebra, one can see that the

use of a position target in Figure 2b, rather than a velocity target in Figure 2a, will elicit the same closed loop behavior given the same trajectory such that P_{target} is the integral of V_{target} (and same controller and aircraft blocks in the model). As such, it should have the same tracking BW. Therefore, in the case of the position target architecture, the phase bandwidth will be extracted at the -45^o frequency of the example longitudinal $\frac{\mathrm{p_x}}{\mathrm{p_{x_{target}}}}(j\omega)$ response, rather than at the traditional -135^0 value used for handling qualities analysis. As shown by the solid line in Figure 5, this results in the same $\omega_{T_{x_{BW}}}$ frequency as the velocity command system, which makes sense given their equivalency. It is worth noting that for a first order response, the -45^o phase bandwidth is equivalent to the -3 db magnitude frequency, which is a common classical definition of bandwidth found in many control systems texts [13].

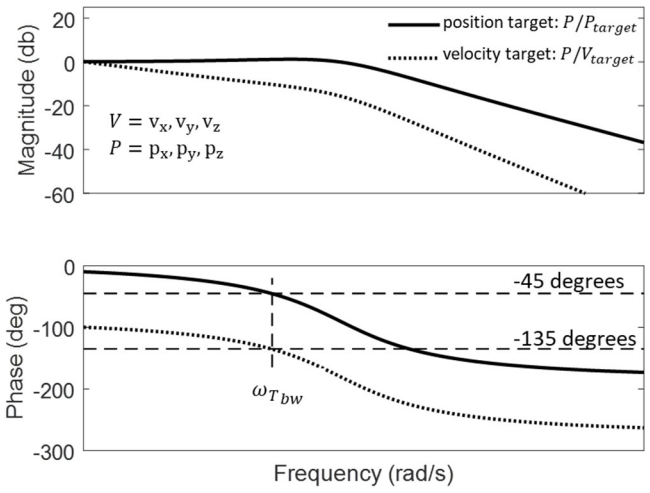

Figure 5. Calculation of tracking bandwidth metric.

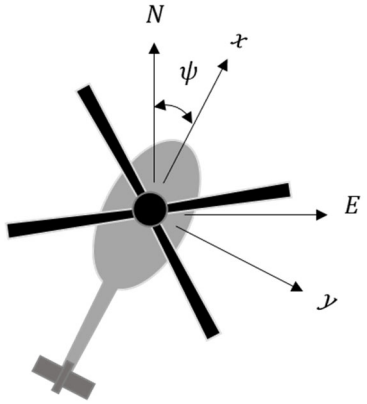

Figure 6. Local vertical (x, y) and Earth (N, E) coordinate frames, z-axis points downward.

CONTROL SYSTEM DESIGN METHODOLOGY

The control systems vary for each of the three test aircraft evaluated in this work; however, each was designed to Froude-scaled ADS-33E-PRF [2] (now superseded by MIL-DTL-32742) attitude BW requirements and MIL-DTL-32742 position and velocity DRB requirements. A key goal of this paper is to validate, at least at small scale, the value of the outer-loop velocity and position metrics as they pertain to automation qualities. Froude scaling of these requirements was completed based on characteristic length, N, which was based on the multicopter hub-to-hub distance or the rotor diameter for a traditional helicopter. The CH-47 Chinook was selected as the full-scale aircraft for Froude scaling purposes, as described in Refs. [14, 4]. The UH-60 is used as the representative full-scale aircraft for the traditional helicopter as described in Ref. [4]. The scaling of the predictive (quantitative) metrics is described fully in Appendix I of this paper.

The control systems were designed to provide parametric variation in velocity and position flying qualities criteria. Note that for all three test aircraft variations of the nested block diagram in Figure 2 were used so that the velocity and position control system architectures are nested around the attitude control loops, such that the bandwidth of the attitude loops inherently affect the velocity and position responses. The following sections describe the control system architectures and design methods that were used to provide a set of control systems with a range of outer loop velocity and position control characteristics for evaluation of MTE performance (and associated automation qualities level) in simulation and flight.

Hexacopter

The UP Hexacopter operates with Arducopter version 4.0 [10], which is used for flight control. Although there are many stock control modes available on ArduPilot, a new control mode was developed by the authors to allow for a custom control architecture. This allowed for a streamlined process where the Simulink block diagram was used in control system design analysis and then processed directly into flight code via Simulink Coder. This custom control system used a nested architecture to follow attitude and trajectory commands, the latter of which was important for performing automated MTEs. This control architecture was also used on prior work [4, 5, 7] for the hexacopter configuration.

The control system design is based on a flight identified model of the aircraft in the mission (heavy) configuration, which is the flight configuration for this paper. The architecture of the control system is quite similar to that of Figure 2a. However, there is an additional inner loop of the attitude-command system that has a dynamic inverse applied in each of the four control axes for improved model following and speed of response. The flight identified model also

provided the A and B matrices for the inverse. The inverted states were $\dot{p}, \dot{q}, \dot{r}$ and $\dot{w}$. Otherwise, the structure follows Figure 2a, with the velocity target command structure, where each block contains the following:

- Attitude Controller Block: 2nd order command model to filter inputs from the velocity control system, with a proportional-integral-derivative controller + lead filter
- Velocity FB Controller Block: proportional-integral controller + lead filter
- Velocity FF Controller Block: not used, set to zero
- Position FB Controller Block: proportional-integral controller
- Acceleration FF Controller Block: not used, set to zero

The architecture is shown in significantly more detail in Refs. [5, 4, 7]. To determine the control system gains used in the inner attitude and outer velocity/position controllers, the set of design specifications, shown in Table 2, were selected and the control system parameters were optimized with CONDUIT® [15] . The requirements in Table 2 are shown in UAS scale to be consistent with how it was implemented in CONDUIT®. Parametric variations in the control system characteristics were made by performing the optimization with a range of positive and negative design margins applied to combinations of attitude BW, velocity DRB and position DRB, so that combinations of L1 and L2 characteristics of each metric could be evaluated to determine which have the highest predictive capability for the MTE performance. Note that tracking BW $\omega_{T_{BW}}$ defined in Table 1 was not specifically used as a CONDUIT® specification, instead was evaluated (check-only) as an output that resulted from variations of attitude BW, velocity DRB, and position DRB.

Seven designs from the design margin optimization were selected, such that a wide range of design characteristics were achieved, as detailed later in Figure 7. All metrics in the Table meet the full-scale L1 requirements except for cases where the design margin was negative to provide parametric variations that intentionally resulted in L2 attitude BW and/or velocity DRB and/or position DRB. All other metrics were held as constant as possible at values at/above the L1/L2 boundary to isolate the effect of the parametric variations.

Synergy 626 and USNTPS X8-M

Both the Synergy 626 and X8-M utilize the stock control system of the Arducopter firmware [10] and were tested in the mission (heavy) configuration. The X8-M simulation utilized a modified version of Arducopter 4.2.3 and the Synergy 626 used a modified version of Arducopter 4.4.4. Both were modified to enable frequency sweeps of commanded velocity, measured velocity and measured position using the System ID mode. The control system consisted of the attitude controller, which provided basic stabilization, and the waypoint and position controllers, which provided the upper-level guidance and navigation. Although code was structured into the separate controllers, the architecture of the control system, overall, is quite similar to that of Figure 2a.

Table 2. Design specifications for pitch/roll axes, reported in UAS scale.

DESIGN SPECIFICATION	CONSTRAINT TYPE	FROUDE SCALED?	INNER LOOP L1/L2 BOUNDARY	OUTER LOOP L1/L2 BOUNDARY
EIGENVALUES	Hard	No	$\lambda \leq 0$	$\lambda \leq 0$
STABILITY MARGINS	Hard	No	GM ≥ 6 dB, PM ≥ 45 deg (inner loop)	GM ≥ 6 dB, PM ≥ 35 deg (outer loop)
MIN CROSSOVER FREQUENCY	Soft	L1/L2 Boundary	$\omega_c \geq$ 12.5 rad/s (at actuator)	$\omega_c \geq$ 12.5 rad/s (at actuator)
ATTITUDE BW	Soft	L1/L2 Boundary	$\omega_{BW} \geq$ 9.31 rad/s	n/a
DRB	Soft	L1/L2 Boundary	$\omega_{DRB_{\phi,\theta}} \geq$ 4.19 rad/s	$\omega_{DRB_{X,Y}} \geq$ 0.79 rad/s $\omega_{DRB_{u,v}} \geq$ 2.51 rad/s
DRP	Soft	No	DRP ≤ 5 dB	DRP ≤ 5 dB
DAMPING RATIO	Soft	Frequency Range	$\zeta \geq 0.35$ (modes $\leq \omega_c$)	$\zeta \geq 0.3$ (modes $\leq \omega_c$)
MODEL FOLLOWING	Soft	Frequency Range	$J_{mf} \leq 50$	n/a
ACTUATOR RMS	Summed Objective	No	Minimize	Minimize
CROSSOVER FREQUENCY	Summed Objective	No	Minimize	Minimize

The waypoint point controller of the Arducopter control system is the trajectory generator shown in Figure 2a. The trajectory from one waypoint to the next was determined using kinematic relations limited by the maximum jerk, acceleration, and velocity parameters specified by the user. The waypoint navigation limits were modified by limitations imposed by the attitude controller command model. In particular, maximum allowable pitch and roll attitudes limited the maximum horizontal acceleration capability of the aircraft.

The position controller was given updated target position and desired velocity and acceleration from the waypoint controller. It generated a thrust vector-based quaternion attitude and level-equivalent heading which was fed to the attitude controller. The position controller used many of the controller blocks in Figure 2a. There were low pass filters in the Velocity FB Controller block. One allowed filtering of the velocity error and the other allowed filtering of the derivative of the velocity error. The type of control used in each block is listed below:

- Velocity FB Controller Block: Proportional-Integral-Derivative Control
- Velocity FF Controller Block: Not used, gain set to zero
- Position FB Controller Block: Proportional Control
- Acceleration FF Controller Block: Proportional Control with gain set to zero or one

The attitude controller was an implicit model following design. It used a command model to shape the commanded attitude into the target response. A time constant parameter was used to define the first order response of the pitch and roll attitude and subsequently the desired rate. An angle feedback controller used a proportional control to provide rate corrections. These rate corrections combined with the desired rate were inputs to the rate controller which consisted of a proportional feedforward control and a Proportional-Integral-Derivative feedback control. The architecture is shown in significantly more detail in Ref. [7].

Initially in the simulation work for the X8-M, waypoint planning was used to set up the MTE course and the waypoint jerk, acceleration and speed settings were used to achieve the desired target velocity profile for a given MTE. Due to the attitude controller having a significant impact on the waypoint controller generated velocity profile, the target velocity profile would change and required unique settings for each attitude controller configuration. This required experimenting with the waypoint controller settings to get similar target velocity profiles between attitude controller configurations. This was tedious and time consuming but tolerable when using simulation. Once testing began with the Synergy 626, this had to be done all through flight testing because a flight-accurate simulation model has not been developed for this aircraft. To alleviate this manual tuning step, the waypoint controller was bypassed and a velocity profile was fed directly into the position controller. This ensured consistent trajectories for all configurations.

The X8-M and Synergy 626 outer loop configurations were manually tuned utilizing the flight test generated commanded attitude to velocity frequency response $\frac{v_y}{\phi_{cmd}}(j\omega)$, combined using frequency response arithmetic with the appropriate outer loop transfer functions from block diagram algebra of Figure 2 to analytically evaluate velocity BW, tracking BW, velocity DRB and DRP, and position DRB and DRP. This proved to be very accurate for the X8-M simulation evaluation, however the configurations needed some adjustments for the actual flight testing of the Synergy 626. Configurations were developed with and without acceleration feedforward path.

The configurations developed for the X8-M simulation study concentrated on investigating a range of outer loop configurations that were wrapped around two different attitude controller designs, one with L1 attitude BW and a second with L2 attitude BW. Each attitude controller met L1 DRB and DRP requirements for attitude. Then two outer velocity/position controllers were designed with the L2 attitude BW controller, one with L1 velocity DRB and another with L2 velocity DRB. Similarly, two outer loop velocity/position controllers were designed with the L1 attitude BW controller, one with L1 velocity DRB and one with L2 velocity DRB. This results in four combinations of attitude BW and velocity DRB. This combination of cases was developed with and without acceleration feedforward (for eight total cases). The specific resulting design metrics for these eight cases are documented later in Figure 7.

Outer loop configurations for the Synergy 626 were developed in a similar manner to the X8-M in that outer loop configurations were developed to meet L1 and L2 velocity DRB and DRP requirements. However, due to the larger separation in the attitude BW configurations (i.e. +/- 20% of the L1/L2 boundary), designing L2 attitude BW cases to meet L1 velocity DRB and DRP requirements was not possible. Therefore, the attitude BW L1/L2 boundary configuration was included as an additional attitude BW configuration and used to achieve this design goal. This was only done with no acceleration feedforward. Only two outer loop configurations were developed with acceleration feedforward in which the L1 attitude BW was used for a L1 velocity DRB configuration and the L2 attitude BW was used for a L2 velocity DRB configuration. There were seven total cases, with design characteristics that are documented in Figure 7 of the next section.

CONTROL SYSTEM CONFIGURATIONS

In order to evaluate the effects and interaction of the outer-loop velocity characteristics and the inner attitude characteristics, a range of cases with varying inner and outer

loop characteristics, as defined in Table 1 were designed as described in the previous control system design methodology section. Figure 7 shows the range of metrics that were designed for each vehicle. On the x-axis is the tracking BW, as this is an important metric that was found in simulation and flight to be a key predictive performance metric. Note that the metrics are scaled to their full-scale equivalent values by dividing by $\sqrt{N}$ for each respective aircraft so the values can be directly compared, where $N = 21.7$ for the hexacopter, $N = 21.4$ for the X8-M, and $N = 12$ for the Synergy 626 helicopter. The dashed lines show the L1/L2 boundary, where values above the dashed line meet the L1 requirement.

The attitude characteristics for the various control designs for the three aircraft are shown in the top two subplots of Figure 7. The attitude BW designs for each aircraft generally fall into two categories, L1 and L2, with a few cases on the L1/L2 boundary for the Synergy 626. The attitude DRB cases were generally designed to meet L1 requirements and all cases are close to the 0.9 rad/s full-scale equivalent boundary, given the very small scale of the y-axis. It should be noted that all of the Synergy 626 cases were slightly into the L2 region for roll attitude DRB requirement of 0.9 rad/s, but did meet the pitch DRB requirement of 0.5 rad/s. A wide range of tracking BW are achieved at each level of attitude BW due to variations in the outer position/velocity control system characteristics.

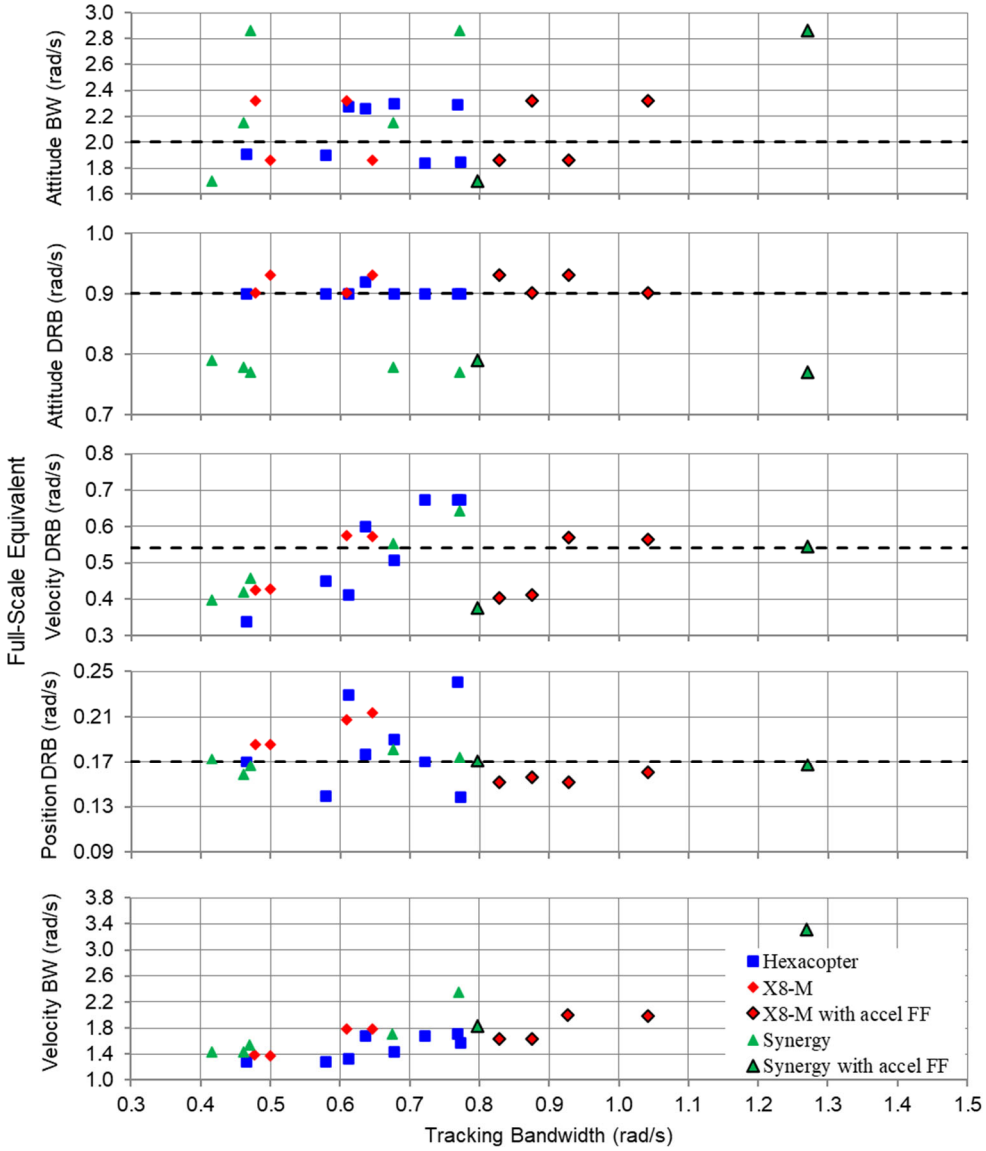

Figure 7. Design cases for the three aircraft, versus full-scale equivalent tracking BW.

The velocity and position characteristics of the system are shown in bottom three subplots of Figure 7. The outer loop control systems were designed to provide a range of velocity and position disturbance rejection characteristics that were above and below the L1/L2 boundary. In some cases, we have a L1 velocity DRB paired with a L1 position DRB, in other cases a combination of L1 and L2, and in some cases both position and velocity DRB values are L2. This was designed to evaluate the effect of each DRB metric independently, and this broad range of cases come with a wide range of tracking BW. In cases without acceleration feedforward, the velocity DRB and tracking BW are correlated as there are no independent feedforward paths. Note that all hexacopter cases have no acceleration feedforward. However, the acceleration feedforward used on the Synergy 626 and X8-M decouples this correlation and increases the tracking BW independent of the velocity DRB as shown by Figure 7. The velocity BW is another metric that was considered and generally trends with the tracking BW, so these two metrics are somewhat related. There are no existing L1/L2 boundaries for the velocity BW or tracking BW as these are newly developed metrics for evaluation in this automation qualities studies and will be evaluated as potential predictive metrics in simulation and flight test within this paper. These new metrics are not defined in MIL-DTL-32742, and as such a proposed L1 requirement will be discussed later in this paper.

The following sections will evaluate the correlation of each of these attitude, velocity and position metrics with the MTE performance, first using flight validated simulation models and then, with flight test data.

SENSITIVITY STUDY IN SIMULATION

The configurations were evaluated in flight-accurate simulation environments for the UP hexacopter and USNTPS X8-M aircraft using lateral reposition automated MTEs within the scaled UAS automation qualities framework (previously known as the UAS handling qualities framework) presented in Ref. [4, 5, 7] and given in the appendix of this paper. The UP hexacopter and USNTPS X8-M aircraft have been shown to have highly flight accurate models in prior work [7]. Because there is no off-axis excitation in simulation and little off-axis coupling present in these vehicles, the key performance indicator of automation qualities level was the maximum on-axis overshoot excursion during the MTE. This is shown in the example lateral reposition MTE for the hexacopter in simulation, shown in Figure 8 as the blue line, with zero off axis excursion and approximately 1.26 ft of on-axis overshoot relative to the hover point at the × mark. Note that the blue aircraft ground track looks like a straight line due to zero off-axis coupling and no disturbances in simulation, but we can see that it overshoots the hover point since the flight path line crosses over the × mark by about 1.26 ft as indicated by the "max excursion" in the inset figure.

The lateral reposition MTE was performed in simulation with no winds or turbulence, for all the X8-M and Hexacopter control system configurations in Figure 7. The results for the maximum (on axis) excursion during the hover capture for each of those cases are given in Figure 9 versus the key predictive metrics of attitude BW, attitude DRB, velocity DRB, position DRB, velocity BW and tracking BW (which were defined in Table 1). The metrics on the x-axes are given in full-scale equivalent values so that all aircraft can be shown on the same scale. All metrics were converted to their full-scale equivalent through Froude scaling laws, by dividing by $\sqrt{N}$ for the associated aircraft ($N = 21.7$ for the hexacopter and $N = 21.4$ for the X8-M). The y-axis excursions are the measured and unscaled values; no scaling is needed because all Group 1 UAS are bound to the same excursion requirements (± 1.35 ft) per Refs. [4, 7] and shown in Appendix II of this paper. As shown in the figure, the strongest predictive metric for the MTE performance is the tracking BW, on the far right. The figure clearly shows that higher tracking BW has a strong trend with improved MTE performance (lower excursions), and vice versa. Considering that this proposed automation qualities metric is not included in MIL-DTL-32742, no L1/L2 boundary exists for this metric, and therefore, no vertical boundary line is shown on the chart. Later in the paper, based on flight test data, a full-scale equivalent boundary of 0.6 rad/s is proposed. The authors also considered the velocity BW metric, which has a similar trend with tracking BW (as shown by the roughly linear relationship in the velocity BW subplot of Figure 7). However, it was not as highly correlated with performance as the tracking BW metric, as shown in Figure 9.

Figure 9 shows DRB is not generally correlated with the performance in simulation, as expected, because there were no gusts or turbulence active in the simulation. We refer to the flight test results later, to provide information regarding the importance of DRB. The figure also shows the surprising result that the correlation in attitude BW was not strong despite contrary evidence shown in Ref. [7], where it was shown to be a good predictive metric. However, in Ref. [7] , care was taken to maintain similar outer loop metrics while varying the inner loop attitude BW. Indeed, the same effect is present for well-performing cases with similar tracking BW circled in the Attitude BW chart, where the higher (L1) attitude BW provides an overall boost in the performance, reducing maximum excursion.

Although there is some correlation with attitude BW, in general, the only metric found in Figure 9 to be a good predictor of performance overall is tracking BW, thus showing the motivation and need for developing a new predictive requirement. One reason this is so effective as a predictive metric is that it includes the effects of feedforward that greatly affect the velocity/position tracking response, but are not captured in the scaled MIL-DTL-32742 velocity and position DRB criteria.

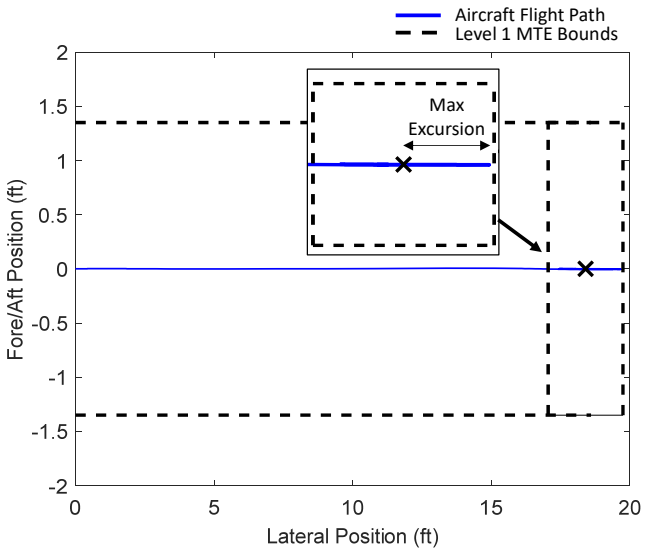

Figure 8. Example lateral reposition simulation data, hexacopter.

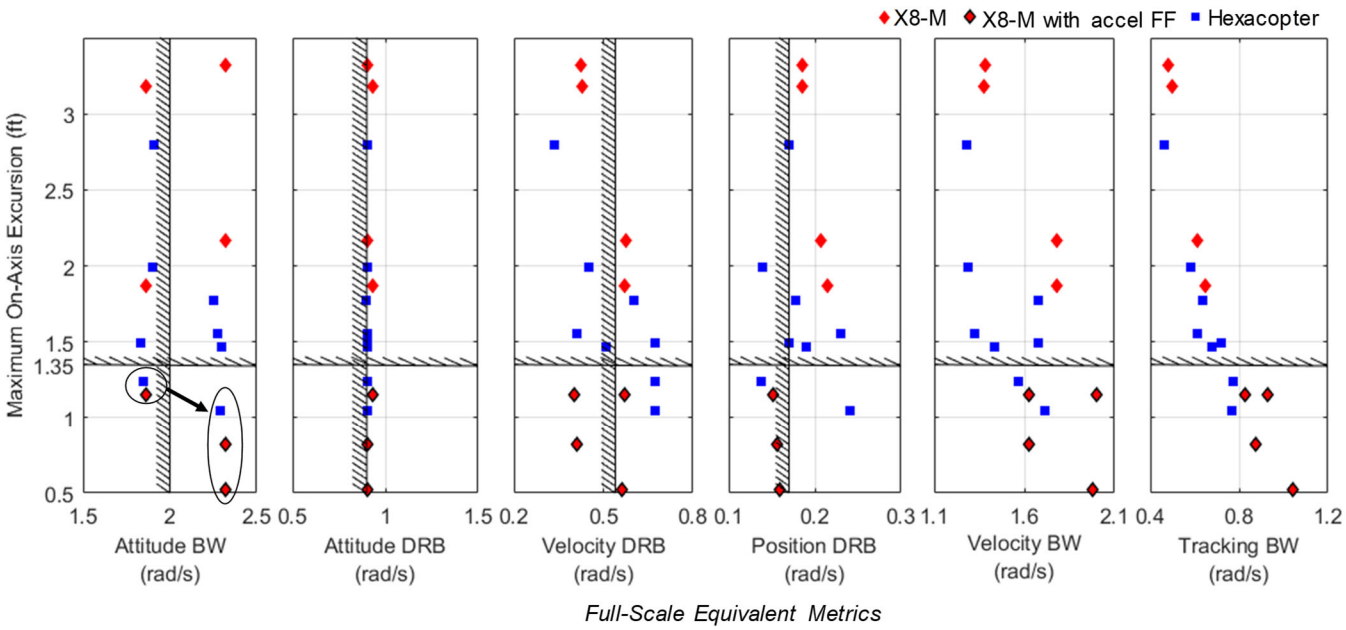

Figure 9. On-axis MTE performance in simulation for lateral reposition.

FLIGHT TEST RESULTS

The flight testing was conducted between January and March of 2024. Hexacopter flights were conducted at the University of Portland and Synergy 626 helicopter flights were conducted in Maryland. The X8-M vehicle was not available for flight test at the USNTPS during the necessary time frame for flight test. Two Froude scaled MTEs, lateral reposition and depart/abort were evaluated in flight test using the scaling and performance standards presented in Ref. [7] and also given in the appendix of this paper. A selection of the control systems from the wide range of configurations presented in Figure 7 were flight tested. Example flight test data for the lateral reposition are shown in Figure 10, showing the difference in performance for cases with the highest and lowest tracking BW for each the hexacopter and Synergy 626 (from Figure 7). Example flight test data for the same two cases on each aircraft for the depart/abort MTE are shown in Figure 11. More comprehensive results of the flight test are presented in Figure 12 for the lateral reposition and in Figure 13 for depart/abort, for all cases and with mean and standard deviation values shown (at least three events were flown for each case). In these figures, the x-axis values are shown at the full-scale equivalent values so that the results can be presented on the same scale and the y-axis excursions are

unscaled (all Group 1 UAS are limited to the same ± 1.35 ft excursion for desired performance in lateral reposition and depart/abort per Appendix II). In both aircraft, the maximum on-axis excursion during the capture portion of the maneuver were found to be more critical than the off-axis excursion (as illustrated by Figure 10 and Figure 11) and was used to evaluate the automation qualities level. For the on-axis excursions, it should be noted that maximum excursion after the time limit was used to evaluate the automation qualities level. This is consistent with the time requirement language for evaluation of the MTEs that is presented in Ref. [7] and given in Appendix I; *overshooting in the on-axis direction of the maneuver is permitted during the deceleration but will show up as a time penalty when the aircraft moves back into the waypoint capture region.* As such, the maximum excursion is evaluated once the scaled time limit, e.g. $18/\sqrt{N}$ seconds for the lateral reposition MTE, has been reached.

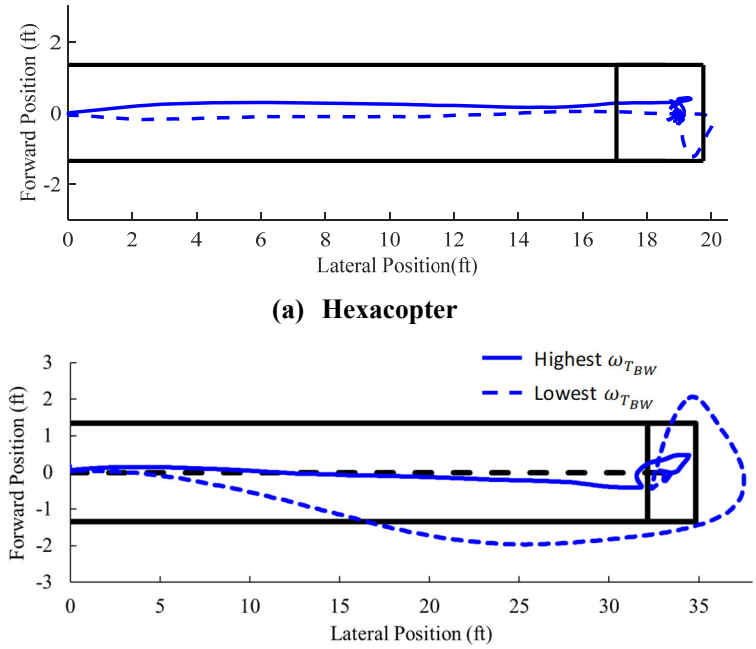

(a) Hexacopter

(b) Synergy 626

Figure 10. Lateral reposition example flight test results.

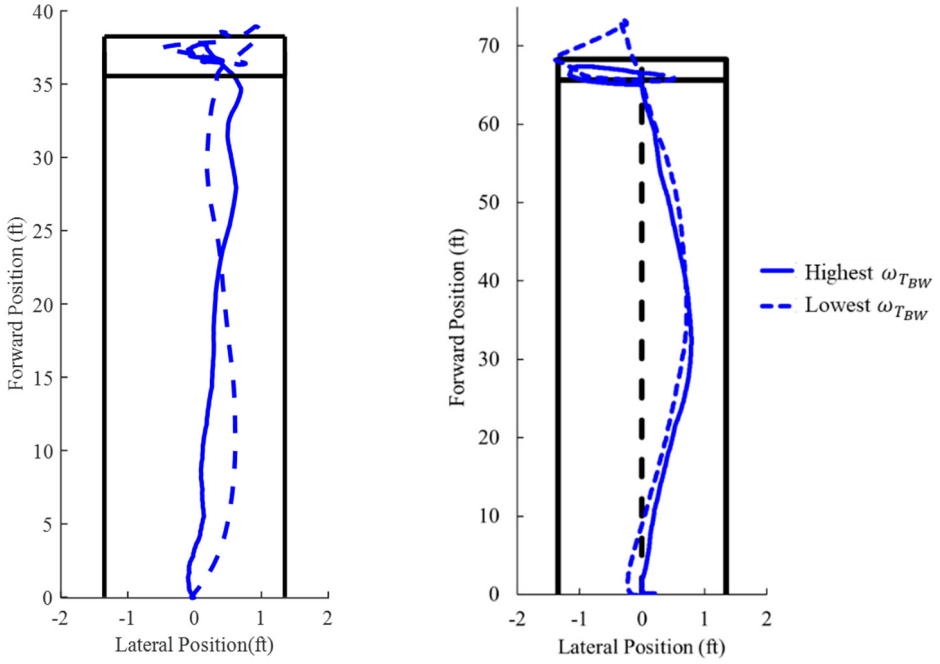

(a) Hexacopter (b) Synergy 626

Figure 11. Depart/abort example flight test results for the hexacopter.

The results for the lateral reposition flight test, in Figure 12, show good correlation with velocity DRB and tracking BW, and correlation with attitude BW was found in most cases as well. This is similar to simulation, where some correlation with attitude BW and high correlation with tracking BW were found. *Based on this data, a proposed Level 1/Level 2 boundary of 0.6 rad/s is proposed for tracking BW.* This proposed boundary is shown on the tracking BW chart on the far right of Figure 12. The simulation did not find correlation with DRB due to lack of disturbances, however, in flight test there is a high correlation with velocity DRB. In the case of the outlier of the tracking BW case, shown with a black hexagon, we can see that the corresponding velocity DRB and attitude BW are in L2. In the case of the strong outlier for the Synergy 626 in the attitude BW plot, shown in a black circle, we can see that the corresponding velocity DRB and tracking BW are also shown in a black circle, in L2. The velocity DRB is a key metric in accurately predicting the performance in both these cases. Another observation from the flight data in Figure 12 is that there was little correlation of performance with position DRB or velocity BW for the lateral reposition MTE. The attitude DRB was largely static and so trends cannot be discerned but have been clearly shown in the other papers [4, 5]. Another trend for cases that have L1 performance is that they largely meet L1 criteria in most of the metrics shown and therefore show the value of designing to a broad set of predictive performance metrics.

The results for the depart-abort cases are shown in Figure 13. In the figure, trends with velocity DRB and tracking BW are again observed, but not as strongly as in the lateral reposition results. The attitude BW was not well correlated with the performance for the depart-abort MTE. However, the position DRB is more correlated with performance for this MTE as compared to lateral-reposition, showing that it is a useful metric. The case shown in the black circle shows the value of the tracking BW, because both attitude BW and velocity DRB are L2 but the L1 tracking BW is consistent with the L1 performance. It is true that this case was flown in low winds, and the authors acknowledge that both high tracking BW and high velocity DRB are needed to result in a good flying case in gusty conditions. However, this case shows that high velocity DRB alone is not sufficient to achieve good performance without good tracking BW, as was also seen in simulation where winds are turned off (Figure 9). The flight results also show that high tracking BW is insufficient without high velocity DRB when disturbances are present, as shown more clearly by the lateral reposition case that was highlighted with the black hexagon in Figure 12. As such, both metrics of velocity DRB and tracking BW are needed to achieve L1 automation qualities in a range of conditions.

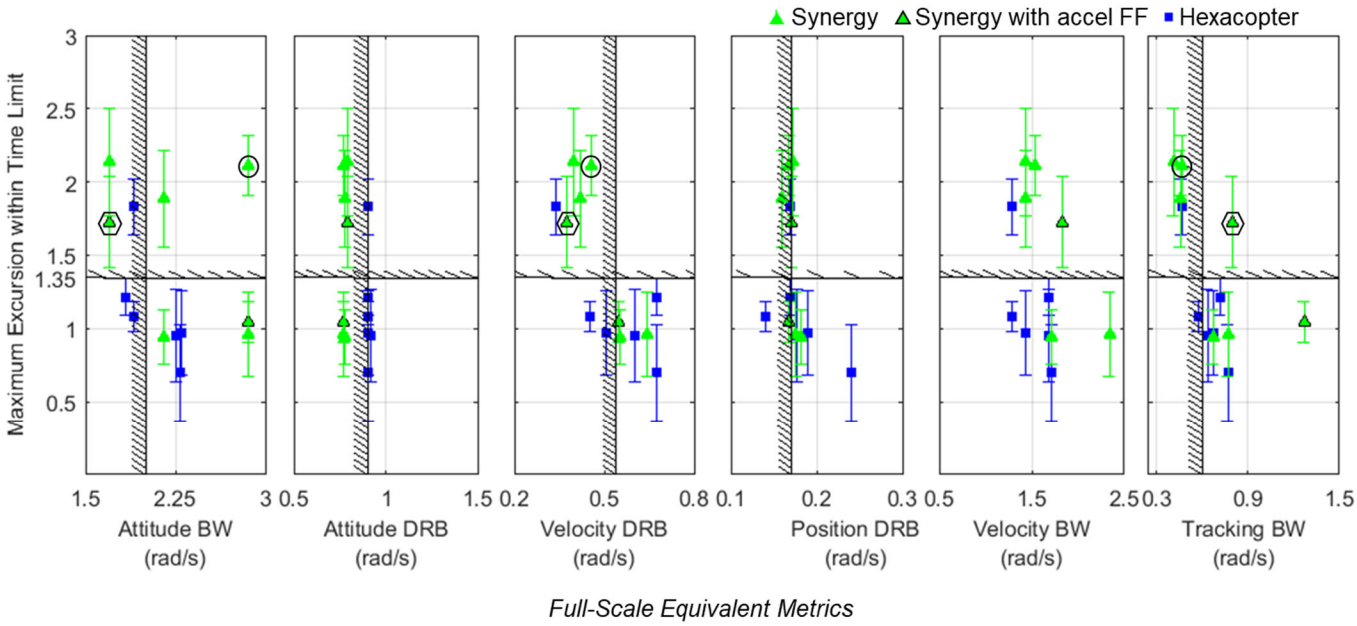

Figure 12. MTE performance in flight for lateral reposition.

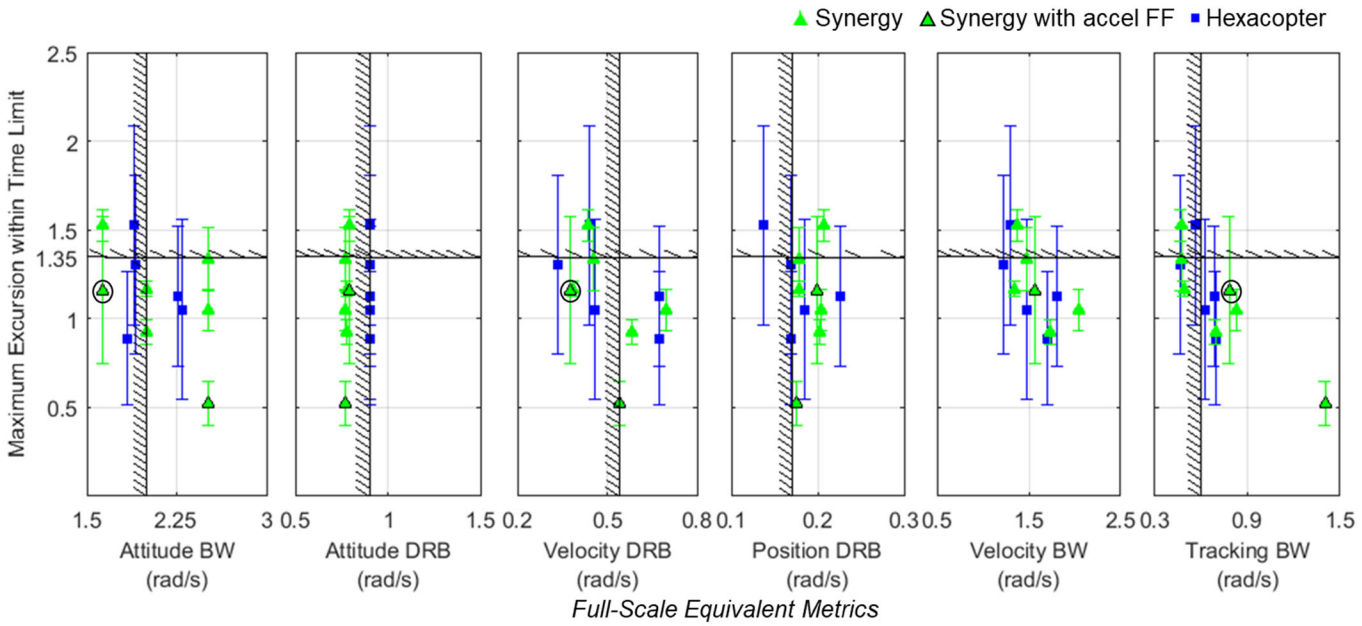

Figure 13. MTE performance in flight for depart/abort.

DISCUSSION

A key result across the MTE results from Figure 12 and Figure 13 are that cases that have most predictive parameters in the L1 region have better performance in general and cases that have more predictive parameters in the L2 region generally have degraded performance. This is consistent with manned handling qualities requirements, where a comprehensive set of predictive metrics are required for L1 handling qualities per MIL-DTL-32742. Additionally, a tiered, comprehensive set of design specifications are typically used for successful control system design, such as in the methods described by Ref. [15]. In the case of unmanned systems, the addition of the tracking BW metric, combined with scaled MIL-DTL-32742 criteria, create a set of metrics required to achieve L1 automation qualities. This is clear from Figure 14, which shows corresponding performance with the number metrics that meet L1 from the bulleted list below:

- Attitude BW (scaled from MIL-DTL-32742)
- Attitude DRB (scaled from MIL-DTL-32742)
- Velocity DRB (scaled from MIL-DTL-32742)
- Position DRB (scaled from MIL-DTL-32742)
- Tracking BW with full scale L1/L2 boundary at 0.6 rad/s (new metric)

When most of these metrics meet L1 (4 or 5), the best performance is achieved, validating the need for these five specifications to be included in the comprehensive set of required criteria for UAS. The authors note that damping and DRP, as well as stability margins were also included in the design selection process and were generally designed to the L1 (unscaled) metrics from MIL-DTL-32742. These metrics are inherently important in any control system and so were considered in the set of design criteria of each control system case but were not varied parametrically. As such, no hard conclusions can be made on the importance of those metrics based on current data, but they are recommended as part of a comprehensive set of design criteria.

It is also worth noting that a good inner loop design that meets attitude BW and DRB requirements is more likely to have good outer loop performance, as it is more difficult (requires additional lead) to design well performing outer (velocity/position) loops around a poorly designed inner attitude loop. For the Synergy 626, it was not possible to achieve a L1 outer velocity/position loop design with a L2 inner attitude loop when the accel FF was turned off. So, designing to this comprehensive set of attitude, velocity and position criteria can also make the L1 design of the outer velocity/position loops more easily achievable.

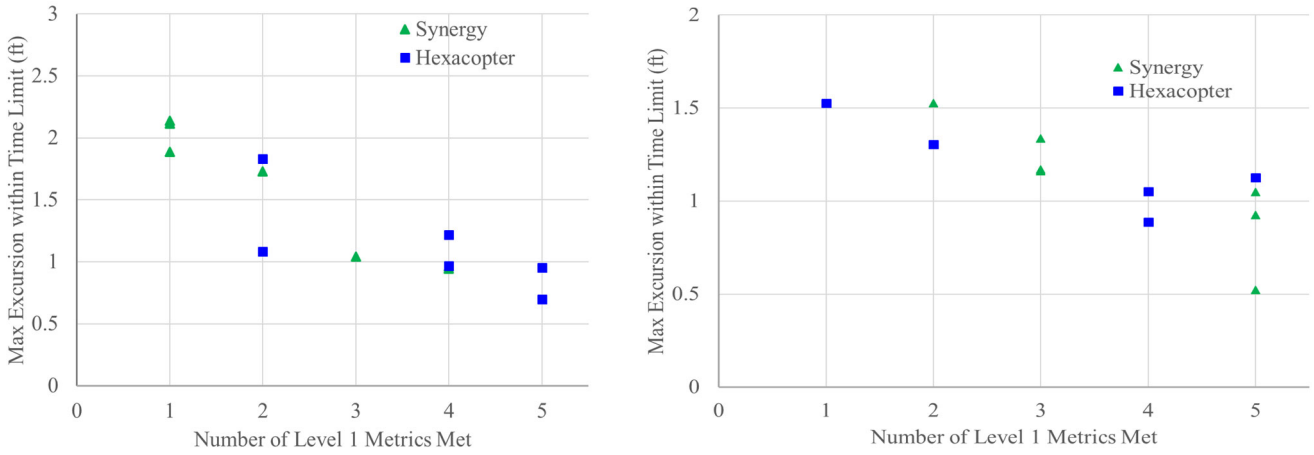

(a) Lateral Reposition **(b) Depart Abort**

Figure 14. Key Level 1 metrics versus MTE performance.

CONCLUSIONS

This paper focused on developing criteria for the UAS automation qualities framework that would provide predictive (quantitative) metrics for velocity and position responses. In prior work, attitude BW and attitude DRB were evaluated as predictive criteria for automation qualities, scaled from MIL-DTL-32742. This work extended that effort by evaluating scaled velocity DRB and position DRB requirements from MIL-DTL-32742, and also evaluated two new metrics; velocity BW and tracking BW. These metrics are defined in the paper and were evaluated as predictive metrics using lateral reposition and depart/abort MTEs. The criteria were evaluated via parametric variation of the control system, with in simulated MTEs for the University of Portland hexacopter and the USNTPS X8-M coaxial quadcopter. Then they were also evaluated via flight test on the University of Portland hexacopter and the Synergy 626 single main rotor helicopter. The following conclusions were made based on the flight test results:

1. The velocity DRB is a key predictive criterion for assigned automation qualities level and the L1/L2 boundary scales well with Froude scaling relative to the full-scale criteria from MIL-DTL-32742.
2. Tracking BW is another important criterion for predicting automation qualities level and should be used in conjunction with the velocity DRB to design the outer velocity/position loops that enable autonomous modes.
3. A full-scale equivalent tracking BW of $\omega_{T_{BW}}$ of 0.6 rad/s is proposed as the L1/L2 boundary for both lateral and longitudinal tracking BW.
4. Control system designs that met L1 requirements for a comprehensive set of five key metrics including attitude BW, attitude DRB, velocity DRB, position DRB and tracking BW tended to provide better MTE performance in flight test evaluation.

ACKNOWLEDGEMENTS

Christina Ivler would like to acknowledge the support of her amazing undergraduate research team in assisting with collection of flight data on the hexacopter. Many thanks to Adam Pua, Austin Law, Connor Possedi, Kayla Medof and Uly Borek.

REFERENCES

[1] Anon, "Department of Defense Detail Specification, Handling Qualities for Military Rotorcraft, MIL-DTL-32742," March 2023.

[2] Anon, "Aeronautical Design Standard, Handling Qualities Criteria For Military Rotorcraft, USAAMCOM, ADS-33E-PRF," US Army, Huntsville, AL, March, 2000.

[3] D. Klyde and e. al., "Towards Handling Qualities and Automation Assessment for Certification of eVTOL Aircraft," in Vertical Flight Society 78th Annual Forum, Fort Worth, TX, May 10-12, 2022.

[4] C. Ivler, K. Russell, A. Gong, T. Berger, Lopez and M. J.S., "Toward a UAS Handling Qualities Specification: Development of UAS-Specific MTEs," in Vertical Flight Society 78th Annual Forum, Dallas-Fort Worth, TX, May 2022.

[5] C. Ivler, K. Troung, K. D., J. Otomize, P. D., N. Gowans and M. Tischler, "Development and Flight Validation of Proposed Unmanned Aerial System Handling Qualities Requirements," in VFS 76th Annual Forum and Technical Display , October, 2020.

[6] C. Ivler, C. Goerzen, J. Wagster IV, F. Sanders, K. Cheung and M. Tischler, "Control Design Tracking of Scaled MTE Trajectories on an IRIS+ Quadcopter," in AHS 74th Annual forum Proceedings , Phoenix, AZ, May, 2017.

[7] C. Ivler, W. Geyer, A. Pua and C. Possedi, "Unmanned Aerial System Handling Qualities Framework Applicability to Heavy Gross Weight Mission-

Configured UAS," in Vertical Flight Society 79th Annual Forum, West Palm Beach, FL, May 16-18, 2023.
[8] C. Blanken, M. Tischler, J. Lusardi, C. Ivler and R. Lehmann, "Proposed Reviews to Aeronautical Design Standard - 33E (ADS-33E-PRF) Toward ADS-33F-PRF," Special Report, FCDD-AMV-19-01, September, 2019.
[9] M. Tischler and R. Remple, Aircraft and Rotorcraft System Identification: Engineering Methods with Flight Test Examples, Reston,VA: AIAA: Education Series, 2012.
[10] "ArduPilot: Copter Home," 2022. [Online]. Available: https://ardupilot.org/copter/. [Accessed 29 September 2022].
[11] "ArduPilot Code Overview," ArduPilot, 2022. [Online]. Available: https://ardupilot.org/dev/docs/apmcopter-code-overview.html. [Accessed 29 September 2022].
[12] M. Tischler, T. Berger, C. Ivler, K. K. Cheung and J. Soong, Practical Methods for Aircraft and Rotorcraft Flight Control Design: an Optimization Based Approach, Reston, VA: AIAA, 2017.
[13] G. Franklin, J. Power and A. Emami-Naeni, Feedback Control of Dynamics Systems, Pearson, 2019.
[14] C. Ivler, K. Truong, D. Kerwin, J. Otomize, D. Parmer, M. Tischler and N. Gowans, "Development and Flight Validation of Proposed Unmanned Aerial System Handling Qualities Requirements," in Vertical Flight Society Annual Forum, 2019.
[15] M. Tischler, T. Berger, C. Ivler, K. Cheung and J. Soong, Practical Methods for Aircraft and Rotorcraft Flight Control Design: An Optimization-Based Approach, Reston, VA: AIAA, 2017.
[16] M. Takahashi and e. al., "Autonomous Guidance and Flight Control on a Partial-Authority Black Hawk Helicopter," Journal of Aerospace Information Systems, vol. 18, no. 10, pp. 686-701, 202

APPENDIX I: AUTOMATION QUALITIES EVALUATION FRAMEWORK

The automation qualities framework (previously known as unmanned handling qualities framework) was developed in Refs. [7, 4, 5] and was designed to be scalable for unmanned systems of many sizes and configurations. The framework includes scalable methods for applying predictive (quantitative) criteria, and it also includes scalable evaluation criteria using scaled MTEs and mission appropriate performance metrics based on UAS group.

I.1 Predicted Automation Qualities Criteria

Predicted handling qualities criteria are available in ADS-33E-PRF. For Group 4 and Group 5 UAS, which are similar in size to full-scale manned rotorcraft, the ADS-33E-PRF predictive criteria can be used directly for the autonomous control system design guidance. For UAS that are smaller than full scale, the criteria can be dynamically Froude-scaled. The scale factor, N is based on the characteristic length. For a multicopter, the characteristic length is the hub-to-hub distance D_{hub}, and for a single main rotor helicopter it is the rotor diameter D_{rotor}. The Froude scaling N is relative to a representative full-scale aircraft, where N indicates $1/N^{th}$ scale:

$$N = \frac{D_{fullscale}}{D_{UAS}} \quad \textbf{1}$$

For metrics involving frequency, Froude scaling indicates that dynamic similarity is achieved by:

$$\omega_{UAS} = \omega_{fullscale}\sqrt{N} \quad \textbf{2}$$

This can be applied to frequency-domain metrics like attitude BW and DRB. Additionally, it can be applied to frequency ranges of interest, such as for example, the frequency range used for application of damping criteria.

For any time-constant based criteria the metric can be scaled as:

$$T_{UAS} = \frac{T_{fullscale}}{\sqrt{N}} \quad \textbf{3}$$

Stability margin requirements and non-dimensional criteria like damping ratio can be applied directly without scaling.

I.2 Evaluation of Assigned Automation Qualities Level

The following framework for determining assigned automation qualities for UAS is proposed. A five-step process, that uses a parallel concept to the process of assigning handling qualities for manned aircraft, is given.

1. Select the intended mission of the UAS

Mission task elements in ADS-33E-PRF are assigned to the applicable categories: scout/attack, utility, and cargo. Similar to this format, the UAS framework will consist of three categories: attack, surveillance/scout, and cargo/delivery.

2. Select the appropriate MTEs for the mission

For each category, a list of MTEs consisting of appropriate scaled ADS-33E-PRF maneuvers and UAS specific maneuvers are assigned. Each MTE in the applicable category can be customized for the appropriate level of aggressiveness as demanded by the mission. The desired MTEs would be selected by the procuring agency. In Appendix I, a detailed description of five MTEs are written in a format similar to ADS-33E-PRF. These five MTEs have been flight validated with Group 1 UAS in prior literature [4].

3. Determine the autonomous trajectories of each MTE via Froude Scaling

After the mission category is selected in Step 2, the MTEs (either ADS-33E-PRF or UAS mission specific) are converted to autonomous trajectories. The MTEs should be scaled with the Froude number to be appropriate for the dynamics of the UAS at hand. The MTE descriptions presented in Appendix I provide the course geometry as a function of N, for ease of use. As an example of how the scaling works, ADS-33E-PRF courses are scaled in length according to the rule:

$$L_{UAS} = \frac{L_{fullscale}}{N} \quad \textbf{4}$$

The velocity and time requirements of the maneuver are also scaled accordingly:

$$V_{UAS} = \alpha \frac{V_{fullscale}}{\sqrt{N}} \quad \textbf{5}$$

$$t_{UAS} = \alpha^{-1} \frac{t_{fullscale}}{\sqrt{N}} \quad \textbf{6}$$

The aggressiveness factor α is nominally equal to one, which provides a scaled acceleration that is equivalent to the original maneuver. Aggressiveness factor $\alpha > 1$ has increased scaled aggression, and likewise, $\alpha < 1$ has less scaled aggression. The option to use an alternate level of aggression is available to provide flexibility to tailor the MTE to the mission requirements. Two levels of aggressiveness (nominal and less aggressive) are evaluated for several MTEs later in the paper.

4. Autonomously fly the MTEs within the time limit at the required level of aggressiveness and evaluate the performance

Once the appropriate trajectory commands are determined in Step 3, they are programmed into the UAS mission planning software or outer-loop control system command. Then, the aircraft will autonomously complete the intended maneuver at the mission-appropriate aggression level. Position tracking, velocity, and time to complete from the maneuver are evaluated against the performance specifications for the MTE. The position tracking requirements are mission-based, not Froude scaled (an explanation is given in the following section). Appendix II provides the flight-validated desired and adequate precision performance metrics for the object avoidance, emergency stop maneuver, and scaled ADS-33E-PRF lateral reposition, depart-abort and pirouette MTEs.

5. Assign an Automation Qualities Level and/or Automation Qualities Rating

After evaluation of the autonomous performance against the MTE, an Automation Qualities Level rating can then be assigned based on the performance of the UAS. Level 1 is assigned for the maneuver if desired performance is met, Level 2 is assigned if adequate performance is met, and Level 3 if adequate performance is not achieved. A modified handling qualities rating scale (for UAS) can be used to refine this into an equivalent Cooper-Harper rating given by the operator if further refinement is needed. The proposed UAS automation (handling) qualities rating scale is given in Ref. [5].

I.3 Method of Evaluating MTE Time to Complete Metrics during Unmanned Trajectories

Several MTEs such as lateral-reposition and depart/abort have desired time to complete metrics and require a stable hover as a condition of completion. One challenge in performing these MTEs autonomously is designing the trajectories to meet the desired time for completion. It is difficult to determine ahead of time how long the stabilization portion of the maneuver will take and hard to know when to call "stable." In order to adapt MTEs to autonomous evaluation and provide a repeatable method to determine the automation qualities level, following language for evaluating the time-to-complete requirement has been proposed:

For desired performance, the unmanned aircraft must achieve the speed requirements for the specified aggressiveness (α) within +/- 5 kts of the full-scale equivalent speed. The UAS shall cross into the final waypoint capture region within the time required to complete. The final hover waypoint should be placed at the center of the capture region, at the end point of the maneuver. Overshooting in the on-axis direction of the maneuver is permitted during the deceleration but will show up as a time penalty when the aircraft moves back into the waypoint capture region.

In summary, the time-to-complete performance is desired if the aircraft is within the capture zone at the time limit and stays within the zone thereafter. As a way to ensure aggressiveness is standardized, the aircraft must achieve the suggested ground speed for the MTE within ± 5 knots of the full-scale equivalent speed (i.e. $\pm 5/\sqrt{N}$ kts). The boundaries of the waypoint capture zone will be given in the course description of applicable MTEs as seen for Depart/Abort and Lateral-Reposition in Appendix I. Although overshooting is not allowed for the ADS-33E-PRF Depart/Abort maneuver, the wording has been updated to allow overshoot for the unmanned version, but with a time penalty, due to difficulty in planning a waypoint-based trajectory that does not overshoot. The goal is to disallow artificial methods of reducing overshoot by placing the final waypoint short of the end point but within the excursion limits.

APPENDIX II: MISSION TASK ELEMENTS

Note that this appendix is identical to that of Ref. [4, 7], but is included here for the convenience of the reader. This appendix presents proposed scaled UAS MTEs presented in the style of ADS-33E-PRF and MIL-DTL-32742. Froude scaling is built into the descriptions of the maneuvers, the performance standards and the autonomous course layouts. The performance standards are provided as a function of UAS group. Group 1 has been tested. Group 2 and Group 3 UAS have not been flight tested, therefore the mission-based performance standards are listed as To Be Determined (TBD). For Group 4 and Group 5, the ADS-33E-PRF MTEs revert back to ADS-33E-PRF courses and standards so they have been considered tested. In the work in Ref [16], ADS-33 MTEs were performed autonomously on a Black Hawk, indicating that these performance standards are achievable for what would be considered a Group 4 UAS.

The following maneuvers are listed in the Appendix:

II.1 Object Avoidance

II.2 Emergency Stop

II.3 Lateral Reposition

II.4 Depart/Abort

II.5 Pirouette

II.0 Froude Scaling of Maneuvers

Scaling is performed relative to a relevant full-scale vehicle, using the characteristic length and the Froude scale N. The following provides guidance on determining an appropriate scale factor N:

- Multicopter: $N = \frac{D_{fullscale}}{D_{hub}}$, where D_{hub} is the hub-to-hub distance of vehicle and $D_{fullscale}$ is the hub-to-hub distance a relevant full-scale multicopter. A suggested value is $D_{fullscale} = 39.2$ ft, based on the CH-47 Chinook.
- Single main rotor: $N = \frac{D_{fullscale}}{D_{rotor}}$, where D_{rotor} is the rotor diameter of the vehicle and $D_{fullscale}$is the hub-to-hub distance of a relevant full-scale helicopter. A suggested value is $D_{fullscale} = 53.7$ ft, based on an H-60 Blackhawk.

Note that if the UAS is "full-scale," meaning it is of similar size to rotorcraft for which ADS-33E-PRF was designed and has been applied then $N = 1$. This will revert to the ADS-33 courses for the autonomous trajectory.

II.1 Object Avoidance

a. Objectives.

- Check ability to maneuver above and below sequential objects.
- Check ability to track a complex trajectory in the longitudinal and vertical axes while flying forward at nap-of -the-earth speeds and maintaining lateral track.

b. Scaling. Scaling is performed using Froude number N relative to an appropriate full-scale vehicle as described in Section I.0 of this Appendix.

c. Description of maneuver. From level fight at an obstacle avoidance speed of approximately $V_{OA} = \frac{30}{\sqrt{N}}$ kts, the aircraft will simulate a forward trajectory that makes changes in altitude to simulate flight over and under obstacles. The UAS will maintain altitude tracking error within the performance requirements relative to the trajectory given in Figure 15 and within lateral tracking standards. The trajectory course length and performance standards do not include the acceleration or deceleration portion of this maneuver.

d. Description of test course. This maneuver requires no physical test course setup as it is autonomous. The course trajectory/waypoints are programmed to complete the maneuver as shown in Figure 15. Performance is evaluated with a reliable positioning system, such as from a differential Global Positioning System (GPS).

e. Performance standards.

Performance standards – Object Avoid

	UAS Group	Desired	Adequate
Maintain lateral track within ± X ft	1	1.35 ft	2.7 ft
	2, 3, 4, 5	TBD	TBD
Maintain altitude tracking error within ± X ft:	1	1.35 ft	2.7 ft
	2, 3, 4, 5	TBD	TBD
Maintain heading within +/- X deg	ALL	10 deg	20 deg
Time to complete maneuver	ALL	$\frac{65}{\sqrt{N}}$	$\frac{80}{\sqrt{N}}$

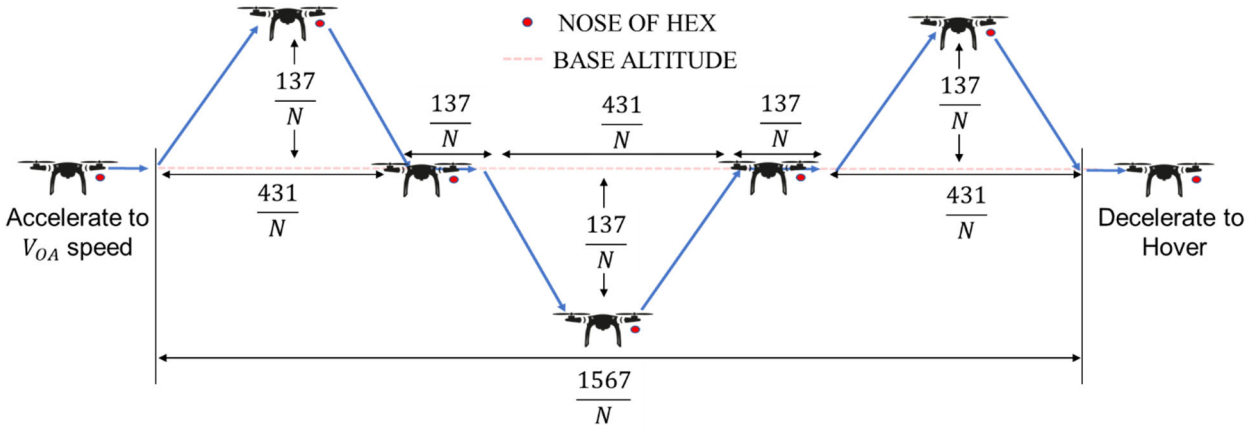

Figure 15. Course trajectory for object avoidance (dimensions are in feet).

II.2 Emergency Stop

a. Objectives.

- Check ability to accomplish an unexpected stop from a representative autonomous operational speed with limited forward distance travel.
- Check ability to maintain altitude when undergoing a rapid, possibly turning deceleration.

b. Scaling. Scaling is performed using Froude number N relative to an appropriate full-scale vehicle as described in Section I.0 of this Appendix.

c. Description of maneuver. From a level flight at a speed of at least V_{decel} knots the aircraft will initiate a rapid deceleration, keeping nose of aircraft forward or completing a turn (coordinated or uncoordinated) as necessary to decelerate with minimal forward travel and maintain altitude. The aircraft will come to a stabilized hover with limited forward travel, while maintaining altitude within the desired limits. The maneuver will end when the aircraft is in a steady hover.

d. Description of test course. This maneuver requires no physical test course setup as it is autonomous. The course trajectory/waypoints are programmed to complete the maneuver as shown in Figure 16. Performance is evaluated with a reliable positioning system, such as differential GPS.

e. Performance standards.

Performance standards - Emergency Stop

	UAS Group	Desired	Adequate
Maintain altitude within $\pm$ X ft	1	1.35 ft	2.7 ft
	2, 3, 4, 5	TBD	TBD
Minimum velocity from which deceleration is initiated, V_{decel}	ALL	$\frac{60}{\sqrt{N}}$ kts	$\frac{50}{\sqrt{N}}$ kts
Maximum allowable forward travel after deceleration is initiated	ALL	$\frac{350}{N}$ ft	$\frac{600}{N}$ ft

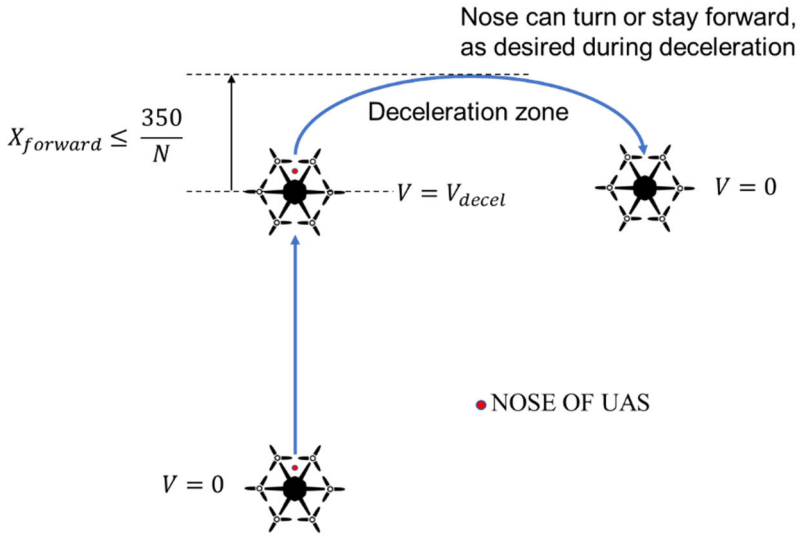

Figure 16. Course trajectory for emergency stop.

II.3 Lateral Reposition

a. Objectives.

- Check roll axis and heave axis automation qualities during a moderately aggressive maneuver
- Check for undesirable coupling between the roll controller and the other axes

b. Scaling. Scaling is performed using Froude number N relative to an appropriate full-scale vehicle as described in Section I.0 of this Appendix.

***c.* Description of maneuver.** Start in a stabilized hover at an appropriate height with the longitudinal axis of the rotorcraft oriented 90 degrees to the desired direction of travel. The autonomous trajectory will initiate a lateral acceleration to a groundspeed of $\frac{35\alpha}{\sqrt{N}}$ kts followed by a deceleration to laterally reposition the UAS to a stabilized hover. *For desired performance at a given α, the UAS much reach this speed within +/- $\frac{5}{\sqrt{N}}$ kts.*

The final hover waypoint should be placed at the 400/N lateral location relative to the start. The UAS shall cross into the final waypoint capture region within the time required to complete. Overshooting is permitted during the deceleration, but will show up as a time penalty when the aircraft moves back into the waypoint capture region. The acceleration and deceleration phases shall be accomplished as single smooth maneuvers.

d. Description of test course. This maneuver requires no physical test course setup as it is autonomous. The course trajectory/waypoints are programmed to complete the maneuver as shown in Figure 17. Performance is evaluated with a reliable positioning system, such as differential GPS.

e. Performance standards.

Performance standards - Lateral Reposition

	UAS Group	Desired	Adequate
Maintain longitudinal track within ± X ft	1	1.35 ft	2.7 ft
	2, 3	TBD	TBD
	4, 5	10 ft	20 ft
Capture and maintain final waypoint laterally within ± Y ft	1	1.35 ft	2.7 ft
	2, 3	TBD	TBD
	4, 5	TBD	TBD
Maintain altitude within ± X ft	1	1.35 ft	2.7 ft
	2, 3	TBD	TBD
	4, 5	10 ft	20 ft
Maintain heading within +/- X deg	ALL	10 deg	10 deg
Time to complete maneuver	ALL	$\frac{18}{\sqrt{N}}$	$\frac{25}{\sqrt{N}}$

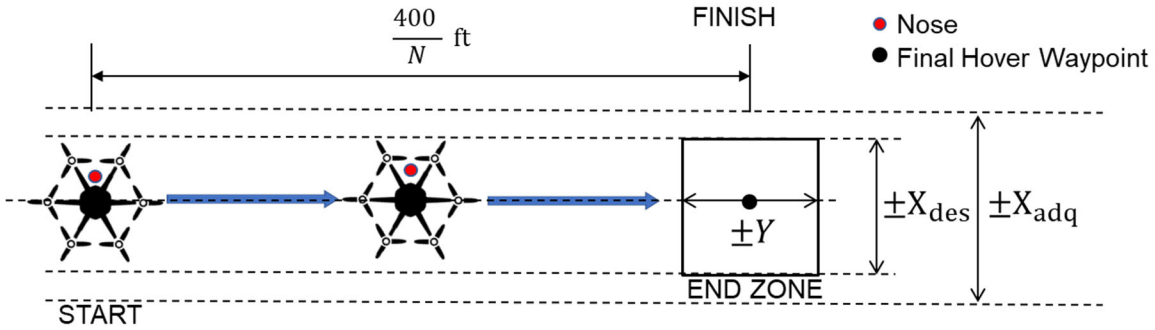

Figure 17. Course trajectory for lateral reposition.

II.4 Depart/Abort

a. Objectives.

- Check pitch axis and heave axis automation qualities during moderately aggressive maneuvering.
- Check for undesirable coupling between the longitudinal and lateral-directional axes.
- Check for ability to re-establish hover after changing trim

b. Scaling. Scaling is performed suing Froude number N relative to an appropriate full-scale vehicle as described in Section I.0 of this Appendix.

c. Description of maneuver. From a stabilized hover at an appropriate altitude, initiate an autonomous longitudinal acceleration to perform a normal departure. At $\frac{45\alpha}{\sqrt{N}}$ kts groundspeed, abort the departure and autonomously begin to decelerate to a hover. *For desired performance at a given α, the UAS much reach this speed within +/-* $\frac{5}{\sqrt{N}}$ *kts.* The final hover waypoint should be placed at the 800/N longitudinal location relative to the start. The UAS shall cross into the waypoint capture zone within the time required to complete. Overshooting is permitted during the deceleration but will show up as a time penalty when the aircraft moves back into the waypoint capture region.

d. Description of test course. This maneuver requires no physical test course setup as it is autonomous. The course trajectory/waypoints are programmed to complete the maneuver as shown in Figure 18. Performance is evaluated with a reliable positioning system, such as differential GPS.

e. Performance standards.

Performance standards - Depart/Abort

	UAS Group	Desired	Adequate
Maintain lateral track within ± Y ft	1	1.35 ft	2.7 ft
	2, 3	TBD	TBD
	4, 5	10 ft	20 ft
Capture and maintain final waypoint laterally within ± X ft	1	1.35 ft	2.7 ft
	2, 3	TBD	TBD
	4, 5	10 ft	10 ft
Maintain altitude within ± X ft	1	1.35 ft	2.7 ft
	2, 3	TBD	TBD
	4, 5	15 ft	40 ft
Maintain heading within +/- X deg	ALL	10 deg	10 deg
Time to complete maneuver	ALL	$\frac{25}{\sqrt{N}}$	$\frac{30}{\sqrt{N}}$

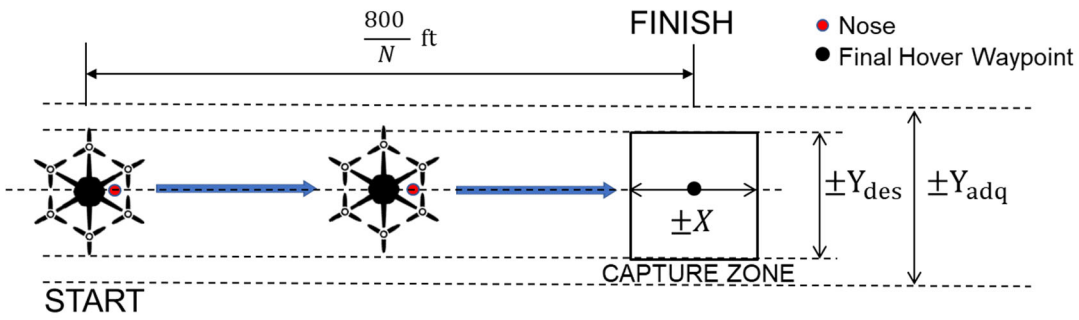

Figure 18. Course trajectory for depart/abort.

II.5 Pirouette

a. Objectives.

- Check ability to achieve precision autonomous control simultaneously in pitch, roll, yaw, and heave.

b. Scaling. Scaling is performed suing Froude number N relative to an appropriate full-scale vehicle as described in Section I.0 of this Appendix.

c. Description of maneuver. Initiate the maneuver from a stabilized hover over a point on the circumference of a $100/N$ ft radius circle with the nose of the UAS pointed at a reference point at the center of the circle, and at an appropriate hover altitude. Accomplish a lateral translation around the circle, keeping the nose of UAS pointed at the center of the circle, and the circumference of the circle under a selected point on the UAS. Maintain essentially constant lateral groundspeed throughout the lateral translation (note: nominal lateral velocity will be approximately $8/\sqrt{N}$ knots for the desired and $6/\sqrt{N}$ knots for adequate time-to-complete.) Terminate the maneuver with a stabilized hover over the starting point. Perform the maneuver in both directions.

d. Description of test course. This maneuver requires no physical test course setup as it is autonomous. The course trajectory/waypoints are programmed to complete the maneuver as shown in Figure 19. Performance is evaluated with a reliable positioning system, such as differential GPS.

e. Performance standards.

Performance standards - Pirouette

	UAS Group	Desired	Adequate
Maintain a selected reference point on the UAS within $\pm$ X ft of the circumference of the circle	1	1.35 ft	2.7 ft
	2, 3	TBD	TBD
	4, 5	10 ft	20 ft
Maintain altitude within $\pm$ X ft:	1	1.35 ft	2.7 ft
	2, 3	TBD	TBD
	4, 5	3 ft	10 ft
Maintain heading such that the nose of the UAS points at the center of the circle within +/- X deg	ALL	10 deg	10 deg
Time to complete maneuver	ALL	$\frac{45}{\sqrt{N}}$	$\frac{60}{\sqrt{N}}$

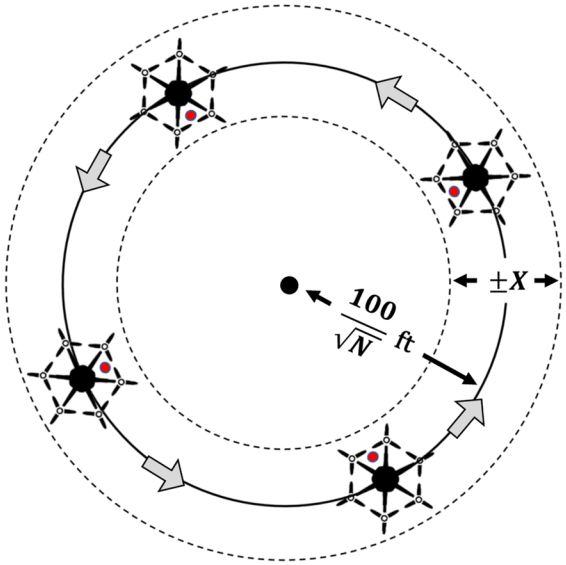

Figure 19. Course trajectory for pirouette.